

# Dynamics of Electric Field Screening in Photoconductive THz Sources with Spatially Patterned Excitation

Dae Sin Kim and D. S. Citrin

Georgia Institute of Technology, School of Electrical and Computer Engineering, Atlanta, Georgia 30332 USA

and

Georgia Tech Lorraine, Technopole Metz 2000 2-3, rue Marconi 57070 Metz, France, Tel :404-894-9916

**Abstract** — We show that the effects of photoinduced screening of the bias field as a function of optical spot shape for ultrafast excitation of photoconductors to generate terahertz radiation using spatially resolve Monte Carlo simulations coupled with a self-consistent Poisson solver. The results of the simulations demonstrate that given the same photoexcited carrier density, a line focus parallel to the direction of the bias field suppresses saturation at high optical fluence due to space-charge screening and enhances the peak terahertz power in the time domain.

## I. INTRODUCTION

Ultrafast broadband THz transients generated by femtosecond optical pulses incident upon biased photoconductors are leading candidates for table-top THz sources. A great effort has been made to improve the performance of such terahertz sources. This performance of THz generation depends on the temporal shape of the photoinduced current pulses and this shape is determined in part by transient velocity overshoot and the screening due to the optically excited electron and hole distributions—space-charge screening as well as dynamic screening associated with the back action of the retarded electromagnetic field [1]-[2]. We investigate the dynamics of photoexcited carrier and screening based on our numerical simulations of the generation of terahertz radiation from photoconductors driven by ultrafast optical pulses with various incident spot shapes through spatially resolved Monte Carlo simulations coupled with a self-consistent Poisson solver. Our simulations demonstrate that considerable control of the emitted terahertz spectrum can be attained by judiciously choosing the optical excitation spot shape on the photoconductor, since the carrier dynamics that provide the source of the terahertz radiation are strongly affected by the ensuing space-charge screening. In particular, for a given initial photoexcited carrier density, by employing a line focus parallel to the bias field, one can largely suppress the effects of screening that tend to cause the terahertz output strength to be saturated.

## II. THE APPROACH

We consider a GaAs-based photoconductive source. The photoconductive switch has two parallel metallic contacts deposited on the surface of a semiconductor as shown in Fig. 1. Patterned on top are assumed to be two

infinitely long parallel electrodes, between which is the photoconductive gap and various laser spot shapes are incident upon this gap that act as carrier sources within the Monte-Carlo simulation as shown in Fig. 1, and the optical excitation is assumed to be Gaussian both temporally and spatially. Most of the terahertz power is generated during the initial ballistic acceleration of the photoexcited carriers. Thus, in order to describe the spatio-temporal response of electrons on a subpicosecond timescale, we compute the carrier distribution function by solving the Boltzmann transport equation[3] from the Monte-Carlo method. In this method, we use acoustic-phonon scattering, ionized-impurity scattering, intervalley scattering, carrier-carrier scattering and screened carrier-phonon scattering[4]-[7] and calculate the screening length self-consistently using the evolving built-in distribution function. We include the three nonparabolic valleys  $\Gamma$ , L, X within the conduction-band and a warped heavy and light-hole band [8]-[10].

When a photoconductor is excited by high peak-fluence optical pulses, the accelerated motion of the electrons by the bias field results in the terahertz radiation, but at the same time, as the carriers undergo their spatial dynamics in the bias field, they partially screen out the bias. The origins of the screening consist of the radiation field and instantaneous space charge-screening, which contribute to the collapse of the total electric field acting

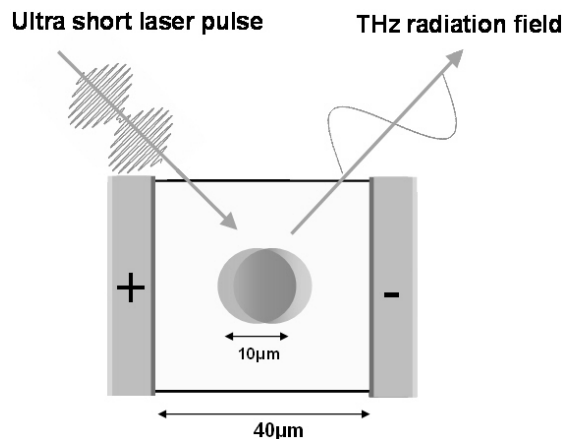


Fig. 1. Schematic diagram of electron (left circle) and hole (right circle) distributions in the biased photoconductor after femtosecond laser excitation.

on the carriers at high carrier density. In order to consider these screening effects, we obtain the retarded terahertz electromagnetic field due to the accelerating carriers [11] as well as longitudinal space-charge screening that builds up as electrons and holes move apart in the bias is considered by the Poisson equation.

For the static screening induced by photoexcited carriers, we consider a GaAs-based photoconductive source laterally biased at 40 kV/cm excited by a 75-fs Gaussian-envelope optical pulse spectrally centered at 800 nm with a repetition rate of 76 MHz for peak excited carrier densities  $10^{17} \text{ cm}^{-3}$ . We use 10,000 superparticles whose distribution is adjusted to be proportional to the temporal and spatial shape of the optical pulse and 900 gridpoints. Patterned on top are assumed to be two infinitely long parallel electrodes, between which is the photoconductive gap with size  $40 \mu\text{m}$ . Laser spot shapes with aperture  $10 \mu\text{m}$  are incident upon this gap as in Fig. 1. This optical excitation act as carrier sources within the Monte-Carlo simulation coupled Poisson solver is assumed to be Gaussian both temporally and spatially. We give simulation results in Fig.2 for electric field profiles after femtosecond laser excitation to understand static screening effects. We can see regions of net positive and negative space charge developed in Fig. 1 as the electrons and holes drift in the opposite direction. The electric field induced by this space charge collapses the bias field as shown in Fig. 2 and results in the saturation of THz output strength.

For the dynamic screening due to the back action of the THz radiation from the accelerating carriers, we obtain the retarded THz electromagnetic field from moving group charges. As is known, the electric field of a point charge  $q$  moving with velocity  $\mathbf{v}$  and acceleration  $\mathbf{a}$  is represented by the formula [11]-[13]

$$\mathbf{E} = \frac{q}{4\pi\epsilon_0} \left( \frac{1}{|1 - \hat{\mathbf{R}} \cdot \mathbf{v}/c|^3} \left\{ \frac{(1 - v^2/c^2)(\hat{\mathbf{R}} - \mathbf{v}/c)}{R^2} + \frac{\hat{\mathbf{R}} \times [(\hat{\mathbf{R}} - \mathbf{v}/c) \times \mathbf{a}]}{c^2 R} \right\} \right)_{rr} \quad (1)$$

where  $\epsilon$  is the permittivity,  $c$  is the velocity of light in photoconductor, and  $\mathbf{R}$  is the radius vector directed from

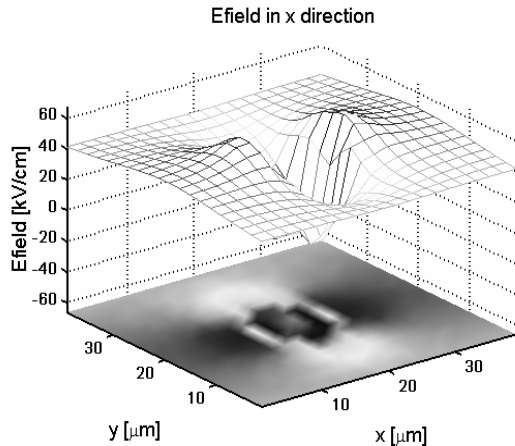


Fig. 2. The static screening field induced by space charge in Fig. 1. It collapses the bias field.

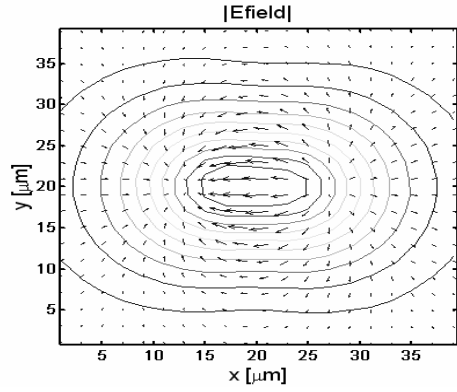


Fig. 3. The direction of THz radiation field on the surface placed  $10 \mu\text{m}$  away from the device.

$q$  to the point of observation.  $\mathbf{R}$ ,  $\mathbf{v}$  and  $\mathbf{a}$  are retarded, that is, evaluated for the time  $t_r = t - R/c$  where  $t$  is the present time for which  $\mathbf{E}$  is evaluated. The magnitude and direction of the electric field at each location is simply the vector sum of the electric field vectors for each individual charge. It is clear that the temporal behavior of the radiated electric field depends directly on the temporal behavior of the velocity and acceleration at an earlier time. The directional characteristics of the radiation field depend upon the relative orientation of the velocity and the acceleration and the near electric field induced by accelerating carriers is in the opposite direction to the bias field and can screen the bias field as shown in Fig. 3.

### III. TRANSPORT PROPERTY

In the following, We consider a photoconductor composed of 30 periods of GaAs/ $\text{Al}_{0.3}\text{Ga}_{0.7}\text{As}$  quantum wells laterally biased with a total thickness of 12 nm excited by a 75-fs Gaussian-envelope optical pulse spectrally centered at 800 nm with a repetition rate of 76 MHz. The velocity of the electrons as a function of time and valley occupancy with different optical spot shapes (spatial spot sizes are  $\sim 10 \mu\text{m}$ ) are plotted in Fig. 4 for an applied field of 40 kV/cm at an excitation level of  $10^{17} \text{ cm}^{-3}$ . For all the optical spot shapes, the excited electrons respond rapidly to the electric field and the velocity increases until a peak value of about  $7 \times 10^5 \text{ m/s}$ ; however, these velocities decrease in a different fashion due to the transfer of the electrons to the upper valleys and screening depending on optical spot shapes. With the spot's major axis perpendicular to the direction of the bias field, the fraction of electrons that transfer to the upper valleys is reduced; in addition, this spot shape leads to a rapid reduction of the electron velocity. This phenomenon occurs due to the interplay of transient velocity overshoot and the strong-space charge screening from the larger net positive and negative space charge. Since this screening field contributes to the collapse of the bias field after fully generation of photocarriers ( $\sim 75 \text{ fs}$ : FWHM optical pulse duration), the electrons do not acquire sufficient energy to access the upper valleys, as a rapid reduction in their velocity due to the strong space-charge screening ensues. By contrast, with the excitation-

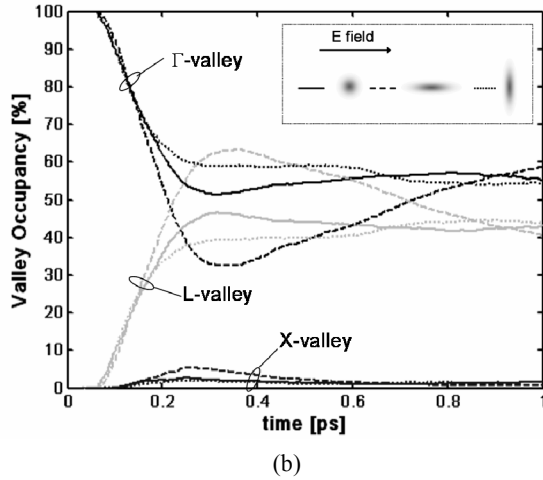
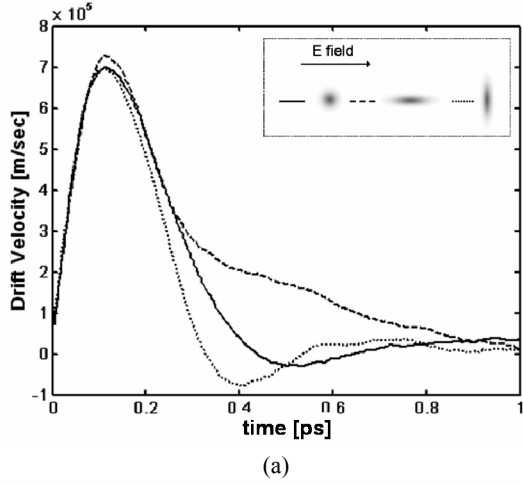


Fig. 4. Drift velocity for photoexcited electrons versus time depending on optical excitation spot shapes, (b) relative electrons occupation of  $\Gamma$ , L and X-valleys versus time at 300 K,  $n=10^{17}\text{cm}^{-3}$ , and 40kV/cm applied bias field.

spot major axis parallel to the direction of the bias field, the electrons reach a peak velocity and then gradually decrease to a saturation velocity as the electrons gradually transfer to the upper valleys. In this case, space-charge screening is relatively weak, with small net positive and negative space charges developing, permitting relatively more carriers to be transferred to the upper valleys. This difference in the resulting electron velocity and acceleration is manifested in the optimization of terahertz radiation, since the total power radiated by the accelerated photocarriers is given by [11]

$$P = \frac{(Nq_{sc})^2}{6\pi\epsilon_0 c^3} \left\{ (1 - v^2/c^2)^{-2} \left[ a^2 + (1 - v^2/c^2)^{-1} (\mathbf{v} \cdot \mathbf{c} \cdot \mathbf{a})^2 \right] \right\}_r, \quad (2)$$

where  $N$  is the number of carriers in the ensemble,  $\mathbf{v}$  and  $\mathbf{a}$  are the retarded ensemble averages of the velocity and acceleration.

Figure 5 shows the peak terahertz power in time domain obtained from Eq. (2) as a function of carrier density for different incident spot shapes excited by a 75 fs optical pulse with a 40 kV/cm applied bias field. The increase in the number of photoexcited carriers enhances the screening field, which suppresses the carrier

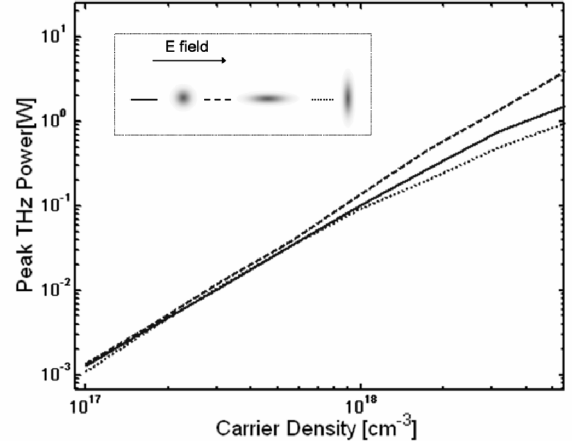


Fig. 5. The terahertz radiation peak power as function of photoexcited carrier density for different spot shape excited by a 75 fs temporal and spatial Gaussian optical pulse at 40 kV/cm applied bias field.

acceleration. This leads to a saturation of the peak terahertz power in time domain. For an elliptical excitation spot with its major axis parallel to the direction of the bias field, however, the instantaneous terahertz power remains essentially linear with input optical power due to the relatively weak space-charge screening and results in a larger peak power than for the circular spot shape, whereas an elliptical excitation spot with its major axis perpendicular to the direction of the bias field leads to saturation of the peak power due to the strong space charge screening.

#### IV. CONCLUSION

To conclude, we have shown that the effects of photoinduced screening of the bias field and the transport properties of the photoexcited carriers in photoconductive THz sources as a function of optical spot shape based on the simulation results. Since the terahertz radiation in the far field is proportional to the time derivative of the current density[14], the emitted terahertz transient depends crucially on the carrier drift velocity. Thus the effects of spatial patterned excitation can be used in order to obtain the temporal velocity profile to produce the desired terahertz transient. One can obtain an enhancement of the terahertz peak power in time domain by judicious choice of the optical excitation spot shape like employing a line focus parallel to the direction of the bias field.

#### REFERENCES

- [1] J. T. Darrow, X.-C. Zhang, D. H. Auston, and J. D. Morse, "Saturation properties of large-aperture photo-conducting antennas," *IEEE J. Quantum Electron.*, vol. 28, pp. 1607-1616, 1992.
- [2] M. Bieler, G. Hein, K. Pierz, and U. Siengner, "Spatial pattern formation of optically excited carriers in photoconductive switches," *Appl. Phys. Lett.* vol. 77, pp. 1002-1004, 2000.
- [3] K. F. Brennan, *The physics of semiconductors with applications to optoelectronic devices*, Cambridge: Cambridge University Press, 1999.

- [4] C. Jacoboni and L. Reggiani, "The Monte Carlo method for the solution of charge transport in semiconductors with applications to covalent materials," *Rev. Mod. Phys.*, vol. 55, pp. 645-705, 1983.
- [5] M. A. Osman and D. K. Ferry, "Monte Carlo investigation of the electron-hole interaction effects on the ultrafast relaxation of hot photoexcited carriers in GaAs," *Phys. Rev. B.*, vol. 36, pp. 6018-6032, 1987.
- [6] W. Fawcett, A. D. Boardman, and S. Swain, "Monte Carlo determination of electron transport properties in Gallium Arsenide," *J. Phys. Chem. Solids*, vol. 31, pp. 1963-1990, 1970.
- [7] J. G. Rush, and W. Fawcett, "Temperature dependence of the transport properties of Gallium Arsenide determined by a Monte Carlo Method," *J. Appl. Phys.* vol. 41, pp. 3843-3849, 1970.
- [8] N. Nintunze, and M. A. Osman, "Hole drift velocity in the warped band model of GaAs," *Semicond. Sci. Technol.* vol. 10, pp. 11-17, 1995.
- [9] T. Brudevoll, T. A. Fjeldly, J. Baek, and M. S. Shur, "Scattering rates for holes near the valence-band edge in semiconductors," *J. Appl. Phys.* vol. 67, pp. 7373-7382, 1990.
- [10] M. T. Portella, J.-Y. Bigot, R. W. Schoenlein, J. E. Cunningham, and C. B. Shank, "k-space carrier dynamics in GaAs," *Appl. Phys. Lett.* vol. 60, pp. 2123-2125, 1992.
- [11] G. S. Smith, *An Introduction to Classical Electromagnetic Radiation*, (Cambridge University Press, Cambridge), pp. 358-376, 1990
- [12] O. D. Jefimenko, "Torque exerted by a moving electric charge on a stationary electric charge distribution," *J. Phys. A: Math. Gen.* vol. 35, pp. 5305-5314, 2002.
- [13] G. S. Smith, "Teaching antenna radiation from a time-domain perspective," *Am. J. Phys.* vol. 69, pp. 288-300, 2000.
- [14] P. K. Benicewicz, J. P. Roberts, and A. J. Taylor, "Scaling of terahertz radiation from large-aperture biased photoconductors," *J. Opt. Soc. Am. B* vol. 11, pp. 2533-2545, 1994.